

# 1 Microbial functional signature in the atmospheric boundary layer

2  
3 Romie Tignat-Perrier<sup>1,2\*</sup>, Aurélien Dommergue<sup>1</sup>, Alban Thollot<sup>1</sup>, Olivier Magand<sup>1</sup>, Timothy  
4 M. Vogel<sup>2</sup>, Catherine Larose<sup>2</sup>

5  
6 <sup>1</sup>Institut des Géosciences de l'Environnement, Université Grenoble Alpes, CNRS, IRD,  
7 Grenoble INP, Grenoble, France

8 <sup>2</sup>Environmental Microbial Genomics, Laboratoire Ampère, École Centrale de Lyon, Université  
9 de Lyon, Écully, France

10  
11 Correspondence to: Romie Tignat-Perrier ([romie.tignat-perrier@univ-grenoble-alpes.fr](mailto:romie.tignat-perrier@univ-grenoble-alpes.fr))

## 12 Abstract

13  
14 Microorganisms are ubiquitous in the atmosphere and some airborne microbial cells were  
15 shown to be particularly resistant to atmospheric physical and chemical conditions (*e.g.*, UV  
16 radiation, desiccation, presence of radicals). In addition to surviving, some cultivable  
17 microorganisms of airborne origin were shown to be able to grow on atmospheric chemicals in  
18 laboratory experiments. Metagenomic investigations have been used to identify specific  
19 signatures of microbial functional potential in different ecosystems. We conducted a  
20 preliminary comparative metagenomic study on the overall microbial functional potential and  
21 specific metabolic and stress-related microbial functions of atmospheric microorganisms in  
22 order to determine whether airborne microbial communities possess an atmosphere-specific  
23 functional potential signature as compared to other ecosystems (*i.e.* soil, sediment, snow, feces,  
24 surface seawater *etc.*). In absence of a specific atmospheric signature, the atmospheric samples  
25 collected at nine sites around the world were similar to their underlying ecosystems. In addition,  
26 atmospheric samples were characterized by a relatively high proportion of fungi. The higher  
27 proportion of sequences annotated as genes involved in stress-related functions (*i.e.* functions  
28 related to the response to desiccation, UV radiation, oxidative stress *etc.*) resulted in part from  
29 the high concentrations of fungi that might resist and survive atmospheric physical stress better  
30 than bacteria.

31  
32 **Keywords:** atmospheric microorganisms, airborne microbial communities, planetary boundary  
33 layer, metagenomic sequencing, comparative metagenomics, selective processes

## 34 1 Introduction

35  
36 Microorganisms are ubiquitous in the atmosphere and reach concentrations of up to 10<sup>6</sup>  
37 microbial cells per cubic meter of air (Tignat-Perrier et al., 2019). Due to their important roles  
38 in public health and meteorological processes (Ariya et al., 2009; Aylor, 2003; Brown and  
39 Hovmøller, 2002; Delort et al., 2010; Griffin, 2007), understanding how airborne microbial  
40 communities are distributed over time and space is critical. While the concentration and  
41 taxonomic diversity of airborne microbial communities in the planetary boundary layer have  
42 recently been described (Els et al., 2019; Innocente et al., 2017; Tignat-Perrier et al., 2019), the  
43 functional potential of airborne microbial communities remains unknown. Most studies have  
44 focused on laboratory cultivation to identify possible metabolic functions of microbial strains  
45 of atmospheric origin, mainly from cloud water (Amato et al., 2007; Ariya et al., 2002; Hill et  
46 al., 2007; Vařtilingom et al., 2010, 2013). Given that cultivatable organisms represent about 1  
47 % of the entire microbial community (Vartoukian et al., 2010), culture-independent techniques  
48 and especially metagenomic studies applied to atmospheric microbiology have the potential to  
49 provide additional information on the selection and genetic adaptation of airborne

50 microorganisms. However, to our knowledge, only five metagenomic studies on airborne  
51 microbial communities at one or two specific sites per study exist (Aalismail et al., 2019; Amato  
52 et al., 2019; Cao et al., 2014; Gusareva et al., 2019; Yooseph et al., 2013). Metagenomic  
53 investigations of complex microbial communities in many ecosystems (for example, soil,  
54 seawater, lakes, feces, sludge) have provided evidence that microorganism functional  
55 signatures reflect the abiotic conditions of their environment, with different relative abundances  
56 of specific microbial functional classes (Delmont et al., 2011; Li et al., 2019; Tringe et al., 2005;  
57 Xie et al., 2011). This observed correlation of microbial community functional potential and  
58 the physical and chemical characteristics of their environments could have resulted from genetic  
59 modifications (microbial adaptation) (Brune et al., 2000; Hindré et al., 2012; Rey et al., 2016;  
60 Yooseph et al., 2010) and/or physical selection. The latter refers to the death of sensitive cells  
61 and the survival of resistant or previously adapted cells. This physical selection can occur when  
62 microorganisms are exposed to physiologically adverse conditions.

63 The presence of a specific microbial functional signature in the atmosphere has not been  
64 investigated yet. Microbial strains of airborne origin have been shown to survive and develop  
65 under conditions typically found in cloud water (*i.e.* high concentrations of H<sub>2</sub>O<sub>2</sub>, typical cloud  
66 carbonaceous sources, UV radiation *etc.*) (Amato et al., 2007; Joly et al., 2015; Vaitilingom et  
67 al., 2013). While atmospheric chemicals might lead to some microbial adaptation, physical and  
68 unfavorable conditions of the atmosphere such as UV radiation, low water content and cold  
69 temperatures might select which microorganisms can survive in the atmosphere. From the pool  
70 of microbial cells being aerosolized from Earth's surfaces, these adverse conditions might act  
71 as a filter in selecting cells already resistant to unfavorable physical conditions. Fungal cells  
72 and especially fungal spores might be particularly adapted to survive in the atmosphere due to  
73 their innate resistance (Huang and Hull, 2017) and might behave differently than bacterial cells.  
74 Still, the proportion and nature (*i.e.* fungi versus bacteria) of microbial cells that are resistant to  
75 the harsh atmospheric conditions within airborne microbial communities are unknown.

76 Our objective was to determine whether airborne microorganisms in the planetary boundary  
77 layer possess a specific functional signature as compared to other ecosystems since this might  
78 indicate that microorganisms with specific functions tend to be more aerosolized and/or  
79 undergo a higher survival in this environment. Our previous study showed that airborne  
80 microbial taxonomy mainly depends on the underlying ecosystems, indicating that the local  
81 environments are the main source of airborne microorganisms (Tignat-Perrier et al., 2019). Still,  
82 we do not know if airborne microbial communities result from random or specific  
83 aerosolization of the underlying ecosystems' microorganisms. We used a metagenomic  
84 approach to compare the differences and similarities of both the overall functional potential and  
85 specific microbial functions (metabolic and stress-related functions) between microbial  
86 communities from the atmosphere and other ecosystems (soil, sediment, surface seawater, river  
87 water, snow, human feces, phyllosphere and hydrothermal vent). We sampled airborne  
88 microbial communities at nine different locations around the world during several weeks to get  
89 a global-scale view and to capture the between and within-site variability in atmospheric  
90 microbial functional potential.

91

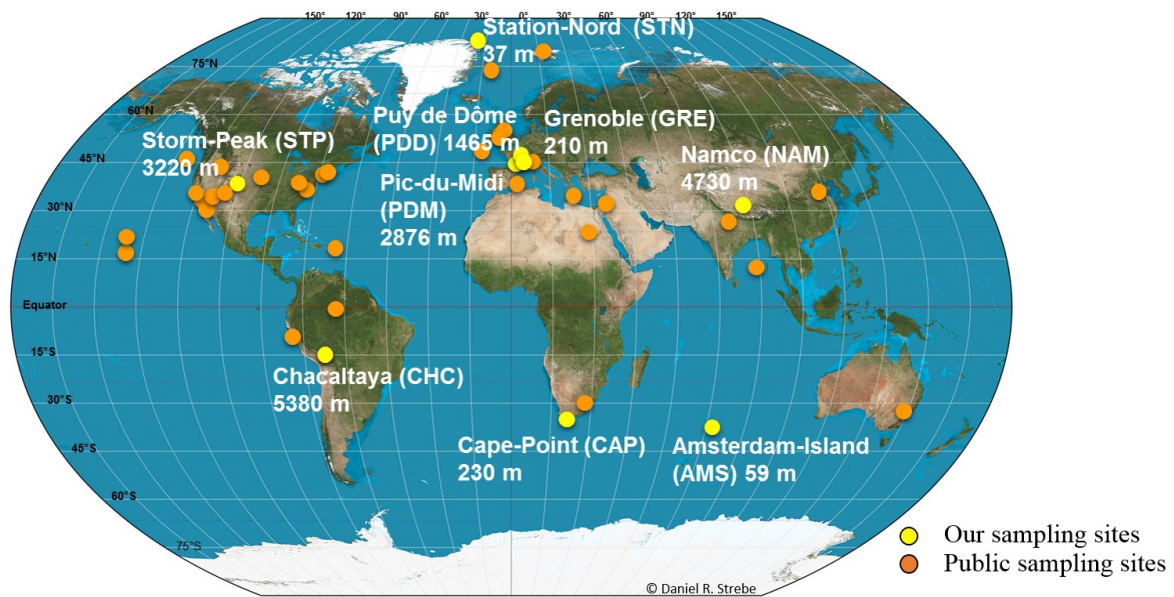
## 92 **2 Material and Methods**

### 93 **2.1 Sites and sampling**

94 Air samples were collected at nine sites in 2016 and 2017. Sites were characterized by different  
95 latitudes (from the Arctic to the sub-Antarctica; **Fig 1**), elevations from sea level (from 59 m to  
96 5230 m; **Fig 1**) and environment type (from marine for Amsterdam-Island or AMS, to coastal  
97 for Cape Point or CAP, polar for Station Nord or STN and terrestrial for Grenoble or GRE,  
98 Chacaltaya or CHC, puy de Dôme or PDD, Pic-du-Midi or PDM, Storm-Peak or STP and  
99 Namco or NAM - **Table S1**). The number of samples collected per site varied from seven to

100 sixteen (**Table S1**). We collected particulate matter smaller than 10  $\mu\text{m}$  (PM10) on quartz fiber  
 101 filters (5.9'' round filter and 8''  $\times$  10'' rectangular types) using high volume air samplers  
 102 (**TISCH, DIGITEL, home-made**) installed on roof tops or terraces (roughly 10 m above ground  
 103 level). To avoid contamination, quartz fiber filters as well as all the material in contact with the  
 104 filters (*i.e.* filter holders, aluminium foils and plastic bags in which the filters were transported)  
 105 were sterilized using strong heating (500  $^{\circ}\text{C}$  for 8 h) and UV radiation, respectively as detailed  
 106 in Dommergue et al., 2019. The collection time per sample lasted one week, and the collected  
 107 volumes ranged from 2000  $\text{m}^3$  to 10000  $\text{m}^3$  after standardization using SATP standards  
 108 (Standard Ambient Pressure and Temperature). Detailed sampling protocols including negative  
 109 control filters are presented in Dommergue et al. 2019. MODIS (Moderate resolution imaging  
 110 spectroradiometer) land cover approach (5'  $\times$  5' resolution) (Friedl et al., 2002; Shannan et al.,  
 111 2014) was used to quantify landscapes in the 50 km diameter area of our nine sampling sites  
 112 (**Fig S1**).

113  
 114



115  
 116 **Fig 1. Sample collection locations.** Map showing the geographical location and elevation from  
 117 sea level of our nine sampling sites (in yellow), and the geographical position of whose public  
 118 metagenomes come from (in orange). Abbreviations of our nine sampling sites are indicated in  
 119 brackets.

120  
 121 **2.2 Molecular biology analyses**

122 **2.2.1 DNA extraction**

123 DNA was extracted from three circular pieces (punches) from the quartz fiber filters (diameter  
 124 of one punch: 38 mm) using the DNeasy PowerWater kit with some modifications as detailed  
 125 in Dommergue et al., 2019. During cell lysis, the PowerBead tube containing the three punches  
 126 and the pre-heated lysis solution were heated at 65  $^{\circ}\text{C}$  during one hour after a 10-min vortex  
 127 treatment at maximum speed. We then separated the filter debris from the lysate by  
 128 centrifugation at 1000 rcf for 4 min. From this step on, we followed the DNeasy PowerWater  
 129 protocol. DNA concentration eluted in 100  $\mu\text{L}$  of buffer was measured using the High Sensitive  
 130 Qubit Fluorometric Quantification (Thermo Fisher Scientific). DNA was stored at -20  $^{\circ}\text{C}$ .

131  
 132 **2.2.2 Real-Time qPCR analyses**

133 **16S rRNA gene qPCR.** The bacterial cell concentration was approximated by the number of  
134 16S rRNA gene copies per cubic meter of air. The V3 region of the 16S rRNA gene was  
135 amplified using the SensiFast SYBR No-Rox kit (Bioline) and the following primers sequences:  
136 Eub 338f 5'-ACTCCTACGGGAGGCAGCAG-3' as the forward primer and Eub 518r 5'-  
137 ATTACCGCGGCTGCTGG-3' as the reverse primer (Fierer et al., 2005) on a Rotorgene 3000  
138 machine (Qiagen). The reaction mixture of 20  $\mu$ L contained 10  $\mu$ L of SYBR master mix, 2  $\mu$ L  
139 of DNA and RNase-free water to complete the final 20  $\mu$ L volume. The qPCR 2-step program  
140 consisted of an initial step at 95 °C for 2 min for enzyme activation, then 35 cycles of 5 s at 95  
141 °C and 20 s at 60 °C hybridization and elongation. A final step was added to obtain a  
142 denaturation from 55 °C to 95 °C with increments of 1 °C s<sup>-1</sup>. The amplicon length was around  
143 200 bp. PCR products obtained from DNA from a pure culture of *Escherichia coli* were cloned  
144 in a plasmid (pCR™2.1-TOPO® vector, Invitrogen) and used as standard after quantification  
145 with the Broad-Range Qubit Fluorometric Quantification (Thermo Fisher Scientific).  
146 **18S rRNA gene qPCR.** The fungal cell concentration was estimated by the number of 18S  
147 rRNA gene copies per cubic meter of air. The region located at the end of the SSU 18S rRNA  
148 gene, near the ITS 1 region, was quantified using the SensiFast SYBR No-Rox kit (Bioline)  
149 and the following primers sequences: FR1 5'-AICCATTC AATCGGTAIT-3' as the forward  
150 primer and FF390 5'-CGATAACGAACGAGACCT-3' as the reverse primer (Chemidlin  
151 Prévost-Bouré et al., 2011) on a Rotorgene 3000 machine (Qiagen). The reaction mixture of 20  
152  $\mu$ L contained 10  $\mu$ L of SYBR master mix, 2  $\mu$ L of DNA and RNase-free water to complete the  
153 final 20  $\mu$ L volume. The qPCR 2-steps program consisted of an initial step at 95 °C for 5 min  
154 for enzyme activation, then 35 cycles of 15 s at 95 °C and 30 s at 60 °C hybridization and  
155 elongation. A final step was added to obtain a denaturation from 55 °C to 95 °C with increments  
156 of 1 °C s<sup>-1</sup>. The amplicon length was around 390 bp. PCR products obtained from DNA from a  
157 soil sample were cloned in a plasmid (pCR™2.1-TOPO® vector, Invitrogen) and used as  
158 standard after quantification with the Broad-Range Qubit Fluorometric Quantification (Thermo  
159 Fisher Scientific).

160

### 161 2.2.3 MiSeq Illumina metagenomic sequencing

162 **Metagenomic library preparation.** Metagenomic libraries were prepared from 1 ng of DNA  
163 using the Nextera XT Library Prep Kit and indexes following the protocol in Illumina's  
164 "Nextera XT DNA Library Prep Kit" reference guide with some modifications for samples with  
165 DNA concentrations below 1 ng as follows. The tagged DNA was amplified over 13 PCR  
166 cycles instead of 12 PCR cycles, and the libraries (after indexing) were resuspended in 30  $\mu$ L  
167 of RBS buffer instead of 52.5  $\mu$ L. Metagenomic sequencing was performed using the MiSeq  
168 and V2 technology of Illumina with 2 x 250 cycles. At the end of the sequencing, the adapter  
169 sequences were removed by internal Illumina software.

170 **Reads quality filtering.** Reads 1 and reads 2 per sample were not paired but merged in a  
171 common file before filtering them based on read quality using the tool FASTX-Toolkit  
172 ([http://hannonlab.cshl.edu/fastx\\_toolkit/](http://hannonlab.cshl.edu/fastx_toolkit/)) using a minimum read quality of Q20, minimum read  
173 length of 120 bp and one maximum number of N per read. Samples with less than 6000 filtered  
174 sequences were removed from the dataset.

175

### 176 2.2.4 Downloading of public metagenomes

177 Public metagenomes were downloaded from the MGRAST and SRA (NCBI) databases as  
178 quality filtered read-containing fasta files and raw read containing fastq files, respectively. The  
179 fastq files containing raw reads underwent the same quality filtering as our metagenomes (as  
180 discussed above). The list of the metagenomes, type of ecosystem, number of sequences and  
181 sequencing technology (*i.e.* MiSeq, HiSeq or 454) are summarized in **Table S2**. The sampling  
182 sites are positioned on the map in **Fig 1**.

183  
184  
185  
186  
187  
188  
189  
190  
191  
192  
193  
194  
195  
196  
197  
198  
199  
200  
201  
202  
203  
204  
205  
206  
207  
208  
209  
210  
211  
212  
213  
214  
215  
216  
217  
218  
219  
220  
221  
222  
223  
224  
225  
226  
227  
228  
229  
230  
231  
232

## 2.3 Data analyses

All graphical and multivariate statistical analyses were carried out using the *vegan* (Oksanen et al., 2019), *ggplot2* (Hadley and Winston, 2019) and *reshape2* (Wickham, 2017) packages in the R environment (version 3.5.1).

### 2.3.1 Annotation of the metagenomic reads

Firstly, to access the overall functional potential of each sample, the filtered sequences per sample were functionally annotated using Diamond, then the gene-annotated sequences were grouped in the different SEED functional classes (around 7000 functional classes, referred simply to as functions) using MEGAN version 6 (Huson et al., 2009). Functional classes that were present  $\leq 2$  times in a sample were removed of this sample. In parallel, the Kraken software (Wood and Salzberg, 2014) was used to retrieve the bacterial and fungal sequences separately from the filtered sequences using the Kraken bacterial database and FindFungi (Donovan et al., 2018) fungal database (both databases included complete genomes), respectively (and using two different runs of Kraken). Separately, both the bacterial and fungal sequences were also functionally annotated using Diamond and MEGAN version 6 (number of sequences functionally annotated in **Table S3**).

Secondly, for specific metabolic and stress-related functions, we annotated the sequences using eggNOG-Mapper version 1 (Diamond option), then examined specific GO (Gene Ontology) terms chosen based on their importance for microbial resistance to atmospheric-like conditions. The different GO terms used were the following: GO:0042744 (hydrogen peroxide catabolic activity), GO:0015049 (methane monooxygenase activity) as specific metabolic functions and GO:0043934 (sporulation), GO:0009650 (response to UV), GO:0034599 (cell response to oxidative stress), GO:0009269 (response to desiccation) as stress-related functions. The number of hits of each GO term was normalized per 10000 annotated sequences and calculated from all sequences, bacterial sequences and fungal sequences for each sample. The number of sequences annotated by eggNOG-Mapper (Huerta-Cepas et al., 2017) was also evaluated (**Table S3**). The putative concentration of a specific function or functional class in the samples is determined as the concentration of sequences annotated as one of the functional proteins associated to this function (or functional class).

### 2.3.2 Statistical analyses

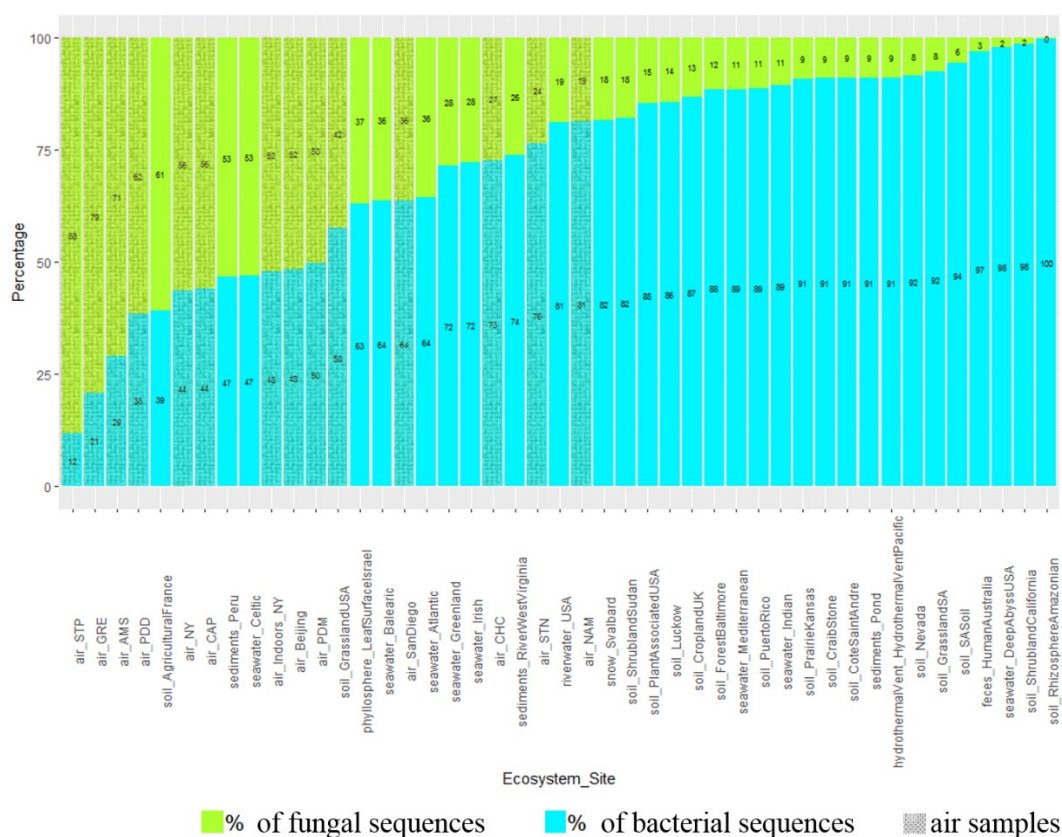
Observed functional richness and evenness were calculated per sample after rarefaction on all sequences (rarefaction at 2000 sequences), bacterial sequences (rarefaction at 500 sequences) and fungal sequences (rarefaction at 500 sequences). The distribution of the samples was analyzed based on the SEED functional classes (using all sequences). PCoA and hierarchical clustering analysis (average method) were carried out on the Bray-Curtis dissimilarity matrix based on the relative abundances of the different SEED functional classes. SIMPER analyses were used to identify the functions responsible for the clustering of samples in groups. Because of the non-normality of the data, Kruskal-Wallis analyses (non-parametric version of ANOVA) and Dunn's post-hoc tests were used to test the difference between the percentage of fungal sequences as well as the number of hits of each Gene Ontology term (normalized per 10000 annotated sequences) among the different sites and the different ecosystems.

## 3 Results

### 3.1 Percentage of fungal sequences

The percentage of sequences annotated as belonging to fungal genomes (or fungal sequences, as opposed to bacterial sequences) was on average higher in air samples compared to soil ( $P < 10^{-5}$ ), snow ( $P = 10^{-3}$ ), seawater ( $P = 0.03$ ) and sediment samples ( $P = 10^{-3}$ ; **Fig 2** and **Table S4**).

233 Among the air samples, NAM (19%), STN (24%) and CHC (27%) showed the lowest  
 234 percentages of fungal sequences on average while STP (88%), GRE (79%), AMS (71%) and  
 235 PDD (62%) showed the highest percentages. For the ecosystems that were only represented by  
 236 one sample, and therefore, were not evaluated by the Kruskal-Wallis test, we observed average  
 237 percentages of fungal reads of 3% in feces, 9% in hydrothermal vents, 19% in river water  
 238 samples and 37% in the phyllosphere. Some samples from soil, sediments and seawater such as  
 239 French agricultural soil (61%), Peru sediments (53%) and Celtic seawater (53%) had relatively  
 240 high percentages of fungal sequences while other samples had less than 50%. The number of  
 241 fungal and bacterial cells was also estimated using 16S rRNA and 18S rRNA gene copy  
 242 numbers per cubic meter of air, respectively. qPCR results on air samples are available in  
 243 Tignat-Perrier et al., 2019. Air samples had ratios between bacterial cell and fungal cell  
 244 concentrations from around 4.5 times up to 160 times lower than soil samples (Table S4).  
 245  
 246

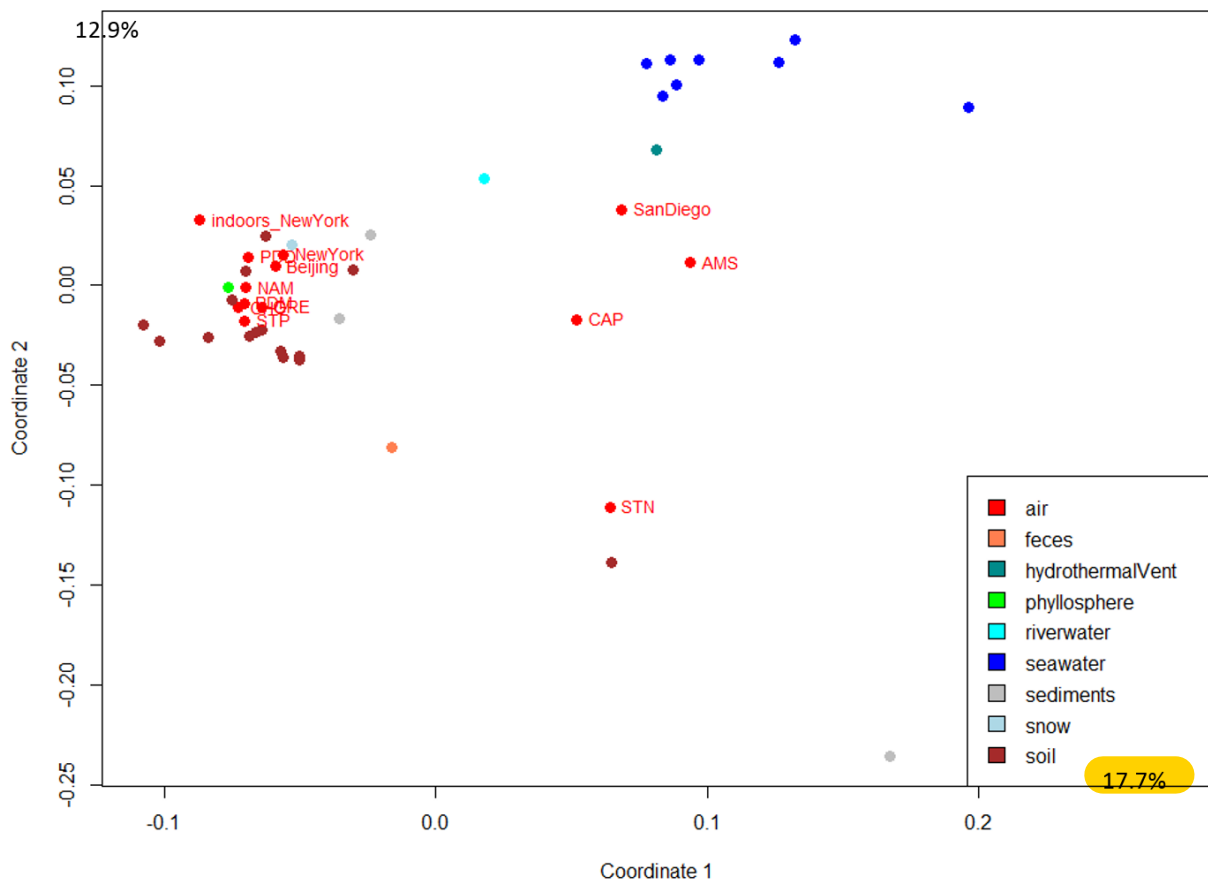


247  
 248 **Fig 2. Percentage of fungal and bacterial sequences in the metagenomes.** The percentages  
 249 are established as the number of sequences annotated as belonging to fungal and bacterial  
 250 genomes over the sum of bacterial and fungal sequences in the metagenomes. The mean was  
 251 calculated for the sampling sites including several metagenomes. Air sites (*i.e.* our 9 sites + 5  
 252 sites where public air metagenomes come from) are distinguished by grey hatching lines.

253  
 254  
 255 **3.2 Airborne microbial functional profiles**

256 The fifty most abundant SEED functional classes represented in atmospheric samples are listed  
 257 in Table S5. The 5-FCL-like protein, the long chain fatty acid CoA ligase and the TonB-  
 258 dependent receptor were the top three functions based on number of annotated reads observed  
 259 when including all the sequences (Table S5). The atmospheric microbial functional profiles

260 based on the SEED functions were compared between samples from the different weeks of  
 261 sampling and between different locations. The profiles were graphed using PCo multivariate  
 262 analysis to visualize differences and similarities. The different samples (sampled during  
 263 sequential weeks) from the same site did not cluster tightly together on the PCo multivariate  
 264 analysis. In order to incorporate weekly variation when comparing sites, we used the microbial  
 265 functional profile averaged per site in the subsequent multivariate analyses done with the data  
 266 from other ecosystems (**Fig 3**). The PCo multivariate analysis showed that terrestrial  
 267 atmospheric sites (GRE, NAM, STP, PDD, PDM, CHC, New York) grouped with the soil,  
 268 sediment and snow samples while the marine and coastal atmospheric sites (AMS, CAP, San  
 269 Diego) were situated between the datasets from soil, seawater and river water (**Fig 3**). The polar  
 270 site STN did not group with the other sites. When considering only the bacterial sequences (*i.e.*,  
 271 excluding the fungal sequences), the distribution of the terrestrial atmospheric sites did not  
 272 change, while the marine Amsterdam-Island, coastal Cape Point and polar Station Nord  
 273 atmospheric sites were further from the seawater and river water datasets than when the fungal  
 274 sequences were included (**Fig S2**). The distribution of the different datasets underwent further  
 275 changes when considering only the fungal sequences. We observed an absence of a clear  
 276 separation between soil and seawater since they (for the majority) grouped closely together, and  
 277 terrestrial atmospheric datasets did not group with the other non-atmospheric datasets from soil,  
 278 sediment and snow (**Fig S2**).  
 279



280  
 281 **Fig 3. Distribution of the samples based on the microbial functional profile.** The PCo  
 282 analysis of the Bray-Curtis dissimilarity matrix is based on the functional potential structure of  
 283 each site. For the site including several metagenomes, the average profile was calculated. Colors  
 284 indicate the ecosystems in which the sites belong to.

285  
286  
287  
288  
289  
290  
291  
292  
293  
294  
295  
296  
297  
298  
299  
300  
301  
302  
303  
304  
305  
306  
307  
308  
309  
310  
311

### 3.3 Airborne microbial functional richness and evenness

Functional richness and evenness were evaluated using the relative abundance of sequences in the different SEED categories. The average richness in SEED functional classes (or functions) in the PBL was lower than the average functional class richness in soil, surface seawater, hydrothermal vents, river water, phyllosphere and feces ( $P<0.05$ ) (**Table S3**). Among the different atmospheric samples, the functional class richness was highest in Beijing (4060 +/- 112 functional classes) and New York indoor air samples (3302 +/- 299 functional classes) ( $P<0.05$ ), and lowest in Station Nord (956 +/- 547 functional classes). When looking at the bacteria-annotated sequences, almost the same trend was observed, *i.e.* the functional class richness in air was lower than in soil, hydrothermal vents, river water, phyllosphere and feces, and not different from the other ecosystems ( $P<0.05$  and  $>0.05$ , respectively) (**Table S3**). The functional class richness was higher in Beijing (2835 +/- 59 functional classes) and New York indoor air samples (2183 +/- 387 functional classes) compared to the other air samples whose values ranged between 270 +/- 197 functional classes in Amsterdam-Island and 1142 +/- 461 functional classes in Chacaltaya. For fungal sequences, the functional class richness in the atmosphere was lower than the functional class richness in soil, surface seawater, feces, hydrothermal vents, river water and phyllosphere ( $P<0.05$ ) (**Table S3**). Within air samples, the functional class richness based on fungal sequences was higher in Beijing (1129 +/- 92 functional classes) and New York indoor air samples (687 +/- 206 functional classes) than in the other air sites ( $P<10^{-5}$ ) whose values ranged from 66 +/- 58 functional classes in Amsterdam-Island and 392 +/- 131 functional classes in Storm Peak (**Table S3**). The functional class evenness in air was on average higher than in soil ( $P=0.03$ ), and not different to the functional class evenness observed in the other ecosystems (sediment, seawater, snow). When looking at the bacterial and fungal sequences separately, the functional class evenness in air was on average higher than in soil, feces, phyllosphere and riverwater ( $P<0.05$ ) (**Table S3**).

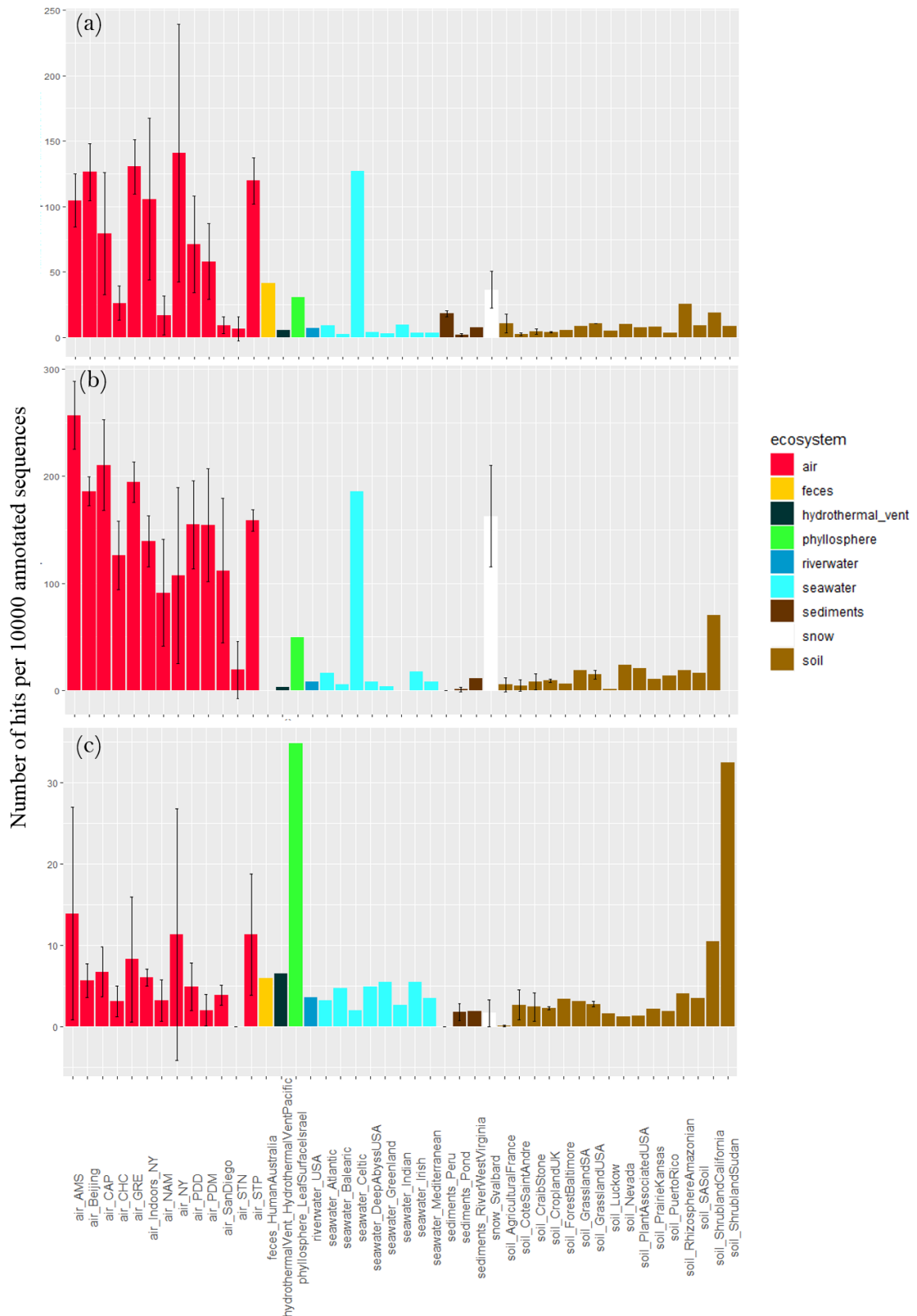
### 3.4 Concentration of specific microbial functions that might have a role under atmospheric conditions

Two metabolic functions associated with abundant atmospheric chemicals ( $H_2O_2$  and  $CH_4$ ) were examined, hydrogen catabolism and methane monooxygenase activity. The concentration of sequences annotated as hydrogen peroxide catabolic related functional proteins per 10000 sequences varied between air sites ( $P=2\times 10^{-5}$ ) with highest values for Amsterdam-Island (27 +/- 1) and Grenoble (27 +/- 1) (**Fig S3**). It was on average higher in air compared to soil ( $P=10^{-4}$ ) and surface seawater ( $P=10^{-4}$ ). The French agricultural soil showed the highest relative abundance (133 +/- 4). When considering the fungal and bacterial sequences separately, this concentration was not different between air and the other ecosystems ( $P>0.05$ ) (**Fig S3**). The number of sequences annotated as methane monooxygenase-related functional proteins per 10000 sequences was only detectable when considering all the sequences (*i.e.* bacterial and fungal sequences). The number of sequences annotated as methane monooxygenase-related functional proteins did not vary between air sites ( $P>0.05$ ) while we observed a high variability between sampling periods within sites, but on average it was not different from the ecosystems ( $P>0.05$ ).

Different stress response functions (sporulation, UV response, oxidative stress cell response, desiccation response, chromosome plasmid partitioning protein ParA and lipoate synthase) were examined. The concentration of sequences annotated as sporulation-related functional proteins per 10000 annotated sequences largely varied between air sites ( $P=2\times 10^{-9}$ ), with the lowest values observed for Station Nord (7 +/- 9), San Diego (9 +/- 6), Namco (17 +/- 15) and Chacaltaya (26 +/- 13), and the highest values observed for Storm Peak (120 +/- 18), Beijing (126 +/- 22), Grenoble (131 +/- 21) and New York (141 +/- 98) (**Fig 4**). It was on average higher



335 in air compared to soil ( $P < 10^{-5}$ ), sediments ( $P < 10^{-5}$ ) and surface seawater ( $P = 4 \times 10^{-4}$ ) although  
336 the Celtic seawater sample presented a very high concentration (127). Snow showed a relatively  
337 high average concentration (*i.e.* 36) which was not different from air concentration ( $P > 0.05$ ).  
338 For the ecosystems including one value (*i.e.* one sample, so not integrated in the Kruskal-Wallis  
339 tests), feces showed a relatively high concentration of sequences annotated as sporulation-  
340 related functional proteins (*i.e.* 41) while hydrothermal vent, phyllosphere and river water  
341 showed relatively low concentrations compared to air ( $< 10$ ). When considering the fungal  
342 sequences separately from the bacterial sequences, the same trend was observed, *i.e.* the  
343 concentration of sequences annotated as sporulation-related functional proteins in air was on  
344 average higher compared to soil ( $P < 10^{-5}$ ), sediments ( $P < 10^{-5}$ ), surface seawater ( $P = 7 \times 10^{-4}$ ) as  
345 well as phyllosphere, hydrothermal vent and river water. The concentration was relatively high  
346 in the Celtic seawater (186) and the snow samples (163 +/- 47). We also observed a large  
347 variability within air sites ( $P = 3 \times 10^{-5}$ ). When considering the bacterial sequences only, this  
348 concentration in air was on average higher compared to soil ( $P = 0.02$ ), sediments ( $P = 4 \times 10^{-3}$ )  
349 and snow ( $P = 0.01$ ), and showed a smaller variability between air sites. Two samples, the  
350 phyllosphere (*i.e.* 35) and the shrubland soil from Sudan (*i.e.* 32) showed high numbers of  
351 sequences annotated as sporulation-related functional proteins per 10000 annotated sequences  
352 (**Fig 4**).  
353



354  
 355  
 356  
 357

**Fig 4. Proportion of sequences annotated as sporulation related functional proteins in the metagenomes.** Average number of sequences annotated as proteins implicated in sporulation per 10000 annotated sequences from (a) all sequences, (b) fungal sequences and (c) bacterial

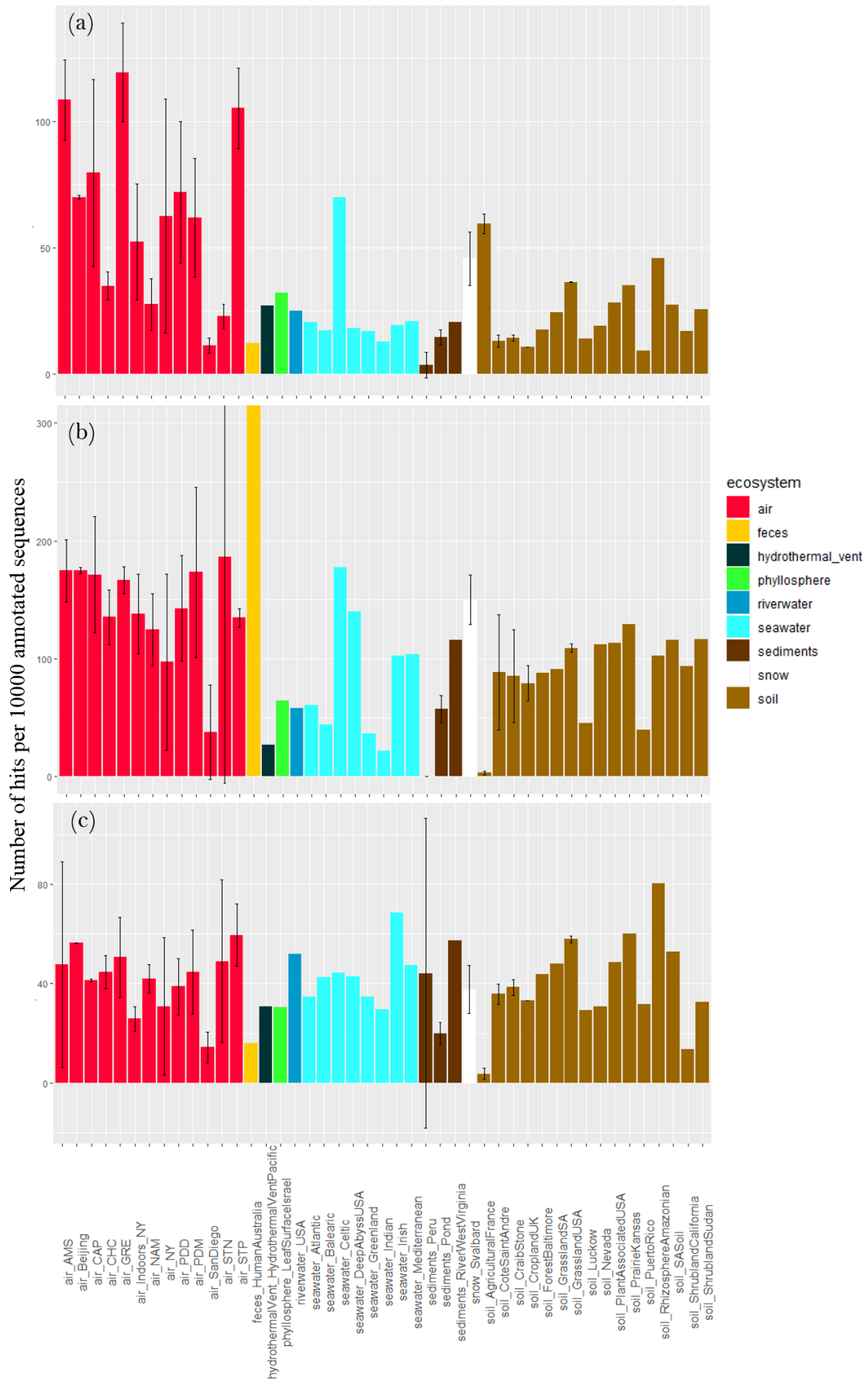
358 sequences per site. Colors indicate the ecosystems in which the sites belong to. For the sites  
359 including several metagenomes, the standard deviation was added.

360

361 The concentration of sequences annotated as UV response related functional proteins per 10000  
362 annotated sequences varied between air sites ( $P=10^{-5}$ ), with values ranging from 16 +/- 2 in  
363 Namco and 19 +/- 4 in STN to 29 +/- 3 in Storm Peak and 36 +/- 6 in Amsterdam-Island (**Fig**  
364 **S4**). The concentration was on average higher in air compared to sediments ( $P<10^{-5}$ ), soil  
365 ( $P<10^{-5}$ ) and comparable to snow and surface seawater ( $P>0.05$ ). The other ecosystems showed  
366 lower ratios (feces, phyllosphere) or comparable concentrations (hydrothermal vent, river  
367 water) compared to air. Within the soil samples, the French agricultural soil samples showed a  
368 high average concentration (56 +/- 8), which increased the average ratio observed in soil  
369 samples. When considering fungal sequences separately, the concentration of sequences  
370 annotated as UV response related functional proteins was higher in air compared to soil  
371 ( $P=9\times 10^{-4}$ ), and comparable to the other ecosystems ( $P>0.05$ ). When considering the bacterial  
372 sequences only, this concentration in air was on average higher compared to seawater ( $P=3\times 10^{-3}$ )  
373 and sediments ( $P=6\times 10^{-3}$ ).

374 The concentration of sequences annotated as oxidative stress cell response related functional  
375 proteins per 10000 annotated sequences varied largely between air sites ( $P=5\times 10^{-7}$ ), with the  
376 lowest values observed for Station Nord (23 +/- 5), San Diego (11 +/- 3) and Namco (28 +/-  
377 10), and the highest values observed for Storm Peak (105 +/- 16), Amsterdam-Island (108 +/-  
378 16) and Grenoble (119 +/- 19) (**Fig 5**). The concentration was on average higher in air compared  
379 to soil ( $P<10^{-5}$ ), sediments ( $P<10^{-5}$ ) and surface seawater ( $P=2\times 10^{-3}$ ). Snow showed a relatively  
380 high average value (46 +/- 11), not different from air ( $P>0.05$ ). The other ecosystems (feces,  
381 river water, hydrothermal vent, phyllosphere) showed lower ratios compared to air. When  
382 considering fungal sequences separately, the concentration of sequences annotated as oxidative  
383 stress related functional proteins per 10000 sequences was on average higher in air compared  
384 to soil ( $P<10^{-5}$ ), sediments ( $P<10^{-5}$ ) and surface seawater ( $P=10^{-3}$ ). Feces showed a very high  
385 average value (2237). When considering bacterial sequences separately, this concentration was  
386 not different between air and the other ecosystems ( $P>0.05$ ). When considering both fungal and  
387 bacterial sequences separately, the variability in the concentration of sequences annotated as  
388 oxidative stress cell response related functional proteins between air sites diminished and their  
389 difference was not detected anymore ( $P>0.05$ ).

390



392 **Fig 5. Proportion of sequences as oxidative stress cell response related functional proteins**  
393 **in the metagenomes.** Average number of sequences annotated as proteins implicated in  
394 oxidative stress cell response per 10000 annotated sequences from (a) all sequences, (b) fungal  
395 sequences and (c) bacterial sequences per site. Colors indicate the ecosystems in which the sites  
396 belong to. For the sites including several metagenomes, the standard deviation was added.

397

398

399 The concentration of sequences annotated as desiccation response related functional proteins  
400 per 10000 sequences varied between air sites ( $P=2\times 10^{-5}$ ), with the highest values in Grenoble  
401 (4 +/- 1), Storm Peak (4 +/- 1) and Amsterdam-Island (3 +/- 3), and the lowest values in Station  
402 Nord (0.5 +/- 1) and San Diego (0.1 +/- 0.1) (**Fig S4**). It was on average higher in air compared  
403 to the other ecosystems ( $P=4\times 10^{-9}$ ). Still Svalbard snow and French agricultural soil showed  
404 high values (2 +/- 1 and 3 +/- 1, respectively) (**Fig S4**). When considering fungal sequences  
405 only, the concentration in air was higher compared to soil ( $P>10^{-5}$ ), sediments ( $P>10^{-5}$ ) and  
406 surface seawater ( $P=10^{-3}$ ). No difference between the ecosystems was observed when  
407 considering bacterial sequences separately ( $P=0.62$ ).

408 Two proteins (lipoate synthase and chromosome plasmid partitioning protein ParA) related to  
409 stress response showed high relative concentrations in bacterial sequences of a few air samples  
410 compared to the other ecosystems (**Fig S3**), although the number of sequences related to these  
411 proteins was on average not higher in the atmosphere than other ecosystems ( $P>0.05$ ).

412

#### 413 **4 Discussion**

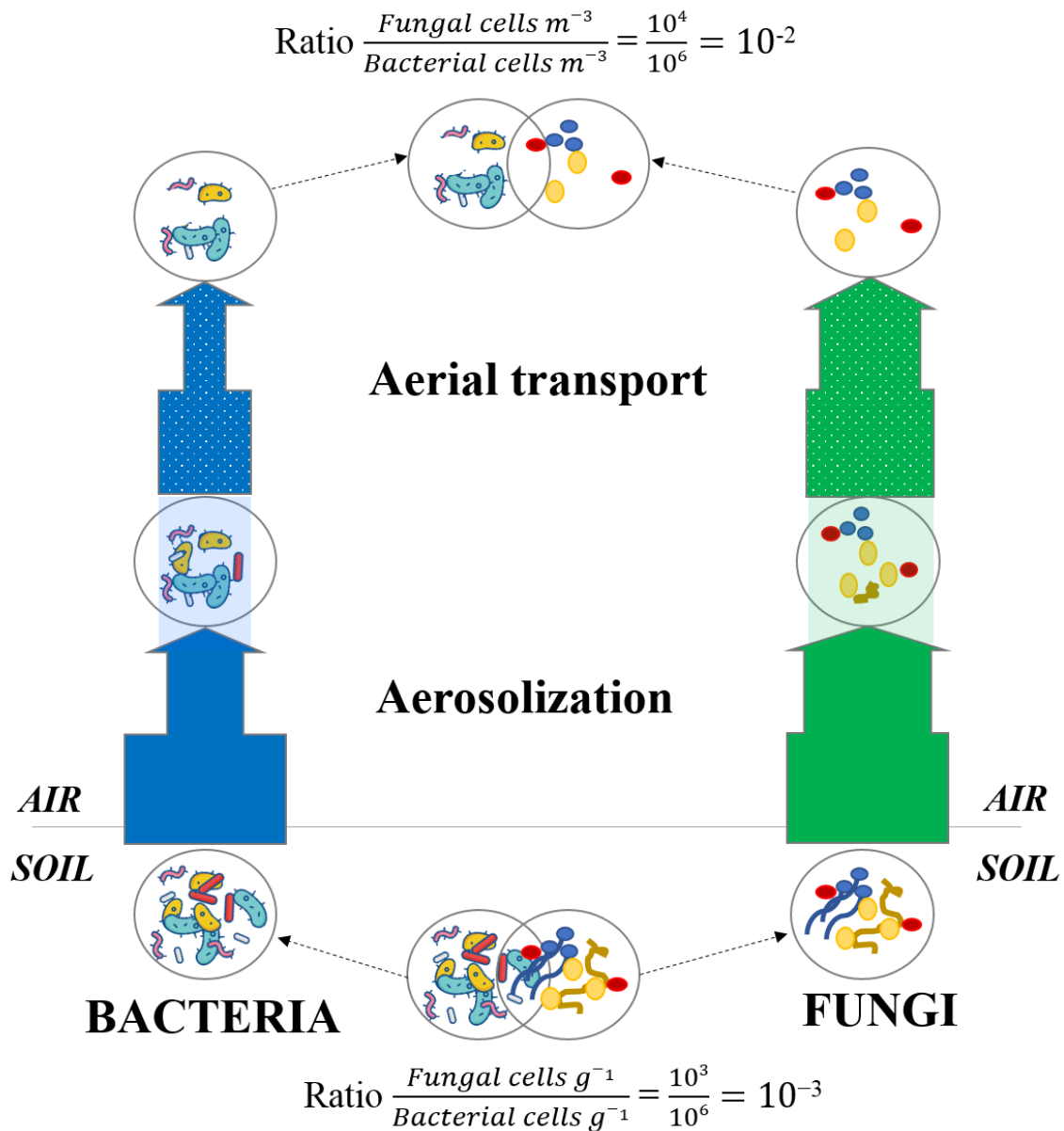
414 Metagenomic investigations of different ecosystems revealed a specific functional potential  
415 signature of their associated microbial communities (Delmont et al., 2011; Tringe et al., 2005).  
416 These specific signatures are thought to result from microbial adaptation and/or physical  
417 selection to the environmental abiotic conditions (Hindré et al., 2012; Li et al., 2019; Rey et al.,  
418 2016) and are a reflection of the high relative abundances of genes coding for specific functions  
419 essential for microorganisms to survive and develop in these environments. For example,  
420 microbial metagenomes of human feces were characterized by high relative abundances of  
421 sequences annotated as beta-glucosidases that are associated with high intestinal concentrations  
422 of complex glycosides; and microbial metagenomes of oceans were enriched in sequences  
423 annotated as enzymes catalyzing DMSP (dimethylsulfoniopropionate), that is an organosulfur  
424 compound produced by phytoplankton (Delmont et al., 2011). Our results showed a clear  
425 separation between surface seawater, river water, human feces and almost all the soil samples  
426 (which grouped with the sediment and snow samples at the scale used here) on the PCo analysis  
427 based on the microbial functional potential (**Fig 3**). For air microbiomes, the PCo analyses  
428 showed that the individual air samples did not group for each site and that they did not form a  
429 cluster separated from the other ecosystems based on the overall microbial functional potential  
430 averaged per site (**Fig 3**). Air samples seemed to group with their underlying ecosystems. While  
431 terrestrial air samples (GRE, NAM, CHC, STP, PDD, PDM) grouped with snow, soil and  
432 sediment samples, the marine (Amsterdam-Island), coastal (Cape Point) and arctic (Station  
433 Nord) air samples were closer to surface seawater and river water samples. Airborne microbial  
434 functional potential (and especially metabolic functional potential as SEED functional classes  
435 included mainly metabolic functions and few stress response related functions) might be  
436 dependent on the ecosystems from which microorganisms are aerosolized. Moreover, it seems  
437 that bacterial sequences are mainly responsible for the distribution of the samples on the PCo  
438 analysis (as observed when comparing the PCoA to that carried out with the fungal sequences  
439 only) although they were in smaller numbers compared to fungal sequences for many of the air  
440 samples (*i.e.* STP, GRE, AMS, PDD, CAP, Beijing *etc.*). The low statistical weight of fungal  
441 sequences relative to the overall sequences might be related to their low richness in terms of

442 functional genes that might have resulted in the spreading of the samples on the PCoA based  
443 on the fungal sequences (**Table S3**).

444 Metagenomes extracted from atmospheric samples taken around the planet were characterized  
445 by a relatively high percentage of fungal sequences as compared to other ecosystems even  
446 though bacterial sequences still dominated. This percentage varied across the different sites  
447 with a higher percentage at terrestrial sites whose surrounding landscapes were vegetated like  
448 Grenoble (GRE), puy de Dôme (PDD) and Pic-du-midi (PDM) (surrounding landscapes in **Fig**  
449 **S1**). This percentage was also relatively high at the marine site Amsterdam-Island (AMS),  
450 where fungi might come from the ocean and/or the vegetated surfaces of the small island. A  
451 high percentage of fungal sequences was also reported for air samples from Beijing, New York  
452 and San Diego and validates our DNA extraction method set-up specifically for quartz fiber  
453 filter (Dommergue et al., 2019). Similarly, the sequencing technology (Illumina MiSeq) could  
454 not have been responsible for the larger percentage of fungal sequences observed in our datasets  
455 as the Beijing and New York/San Diego air sample datasets originated from Illumina HiSeq  
456 and 454 sequencing technology, respectively. qPCR results on the 16S rRNA gene (bacterial  
457 cell concentration estimation) and on the 18S rRNA gene (fungal cell concentration estimation)  
458 on our air samples in comparison to soil samples (Côte Saint André, France) showed that the  
459 ratio between fungal and bacterial cell number was much higher (from 4.5 to 160 times higher  
460 for the most vegetated site Grenoble) in air than in soil (**Table S4**). The ratio between fungal  
461 and bacterial cell number might be higher in the planetary boundary layer (PBL) than in other  
462 environments like soil (Malik et al., 2016), and thus, would explain the relatively higher  
463 percentage of fungal sequences observed in air metagenomes. High throughput sequencing  
464 allows the sequencing of a small part of the metagenomic DNA (with large fungal genomes  
465 likely to be sequenced first) and might explain why the values of the bacteria and fungi  
466 abundance ratio obtained by qPCR does not match those obtained by the metagenomic  
467 sequencing approach. Our study is a preliminary metagenomic investigation of the air  
468 environment with a limited number of sequences per sample, and further studies are needed to  
469 confirm our results.

470 Fungi in the atmosphere are expected to be found mostly as fungal spores, although the relative  
471 concentration of fungal spores and fungal hyphae fragments in air is unknown. Our results  
472 showed that the number of sporulation-related functions was higher in air than the other  
473 ecosystems (with the exception of snow and phyllosphere). While fungal hyphae are not  
474 expected to be particularly resistant to extreme conditions such as UV radiation, fungal spores  
475 are specifically produced to resist and survive overall adverse atmospheric conditions (Huang  
476 and Hull, 2017). Their thick membrane and dehydrated nature make them particularly resistant  
477 to abiotic atmospheric conditions such as UV radiation, oxidative stress, desiccation as well as  
478 osmotic stress. **Fig 6** presents a conceptual model that could explain the higher ratio between  
479 fungi and bacteria observed in air. During aerosolization and aerial transport, bacteria and fungi  
480 might be under stress and might undergo a physical selection with the survival of the most  
481 resistant cells to the adverse atmospheric conditions (*i.e.* UV radiation, desiccation *etc.*) and the  
482 death of non-resistant cells. As fungi (and especially fungal spores) might be naturally more  
483 resistant and adapted to atmospheric conditions than bacteria, we expect a larger decline of  
484 bacterial cells compared to fungal cells and spores in air. This might have as a consequence an  
485 increase in the ratio between fungi and bacteria compared to their non-atmospheric origins (*i.e.*  
486 the surrounding ecosystems) (**Fig 6**).

487



488  
 489  
 490  
 491  
 492  
 493  
 494  
 495  
 496  
 497

**Fig 6. Microbial cell loss due to atmospheric physical stress.** Conceptual model on the microbial cell loss occurring during the aerosolization and aerial transport steps due to physical selection. The thickness of the arrows represents the impact of the physical selection on both bacterial and fungal cell loss (the more microbial cells survive the physical selection, the thicker becomes the arrow). Approximate ratios are indicative and result from 16S rRNA and 18S rRNA qPCR data on Côte Saint André soil samples (crop soil, France) and puy de Dôme air samples (France; puy de Dôme landscape is mainly composed of croplands as shown in **Fig S1**).

498  
 499  
 500  
 501  
 502  
 503

The high variability between the air sites and between air samples of the same site could be explained by the variability in the inputs from the different surrounding landscapes. Our previous paper showed that local inputs were the main sources of planetary boundary layer microorganisms and that local meteorology (especially the wind direction) had a major impact on the temporal variability of airborne microbial communities by affecting which of the

504 different local sources were upwind (Tignat-Perrier et al., 2019). Our results did not show a  
505 specific (metabolic) functional potential signature for the atmosphere, which was rather mainly  
506 driven by the surrounding landscapes. Our results are consistent with both a pre-metabolic  
507 adaptation of airborne microorganisms to the chemicals of the sources (*i.e.* surrounding  
508 landscapes) and a potential metabolic adaptation to these chemicals in the atmosphere.

509 Atmospheric chemistry is dependent on the underlying ecosystem chemistry since the main  
510 sources of atmospheric chemicals are Earth surface emissions. Yet, the oxidizing conditions of  
511 the atmosphere might lead to rapid transformations of atmospheric chemicals by photochemical  
512 reactions. These specific atmospheric chemical reactions (*i.e.* photochemical) produce species  
513 which, with the gases like CH<sub>4</sub>, characterize the atmosphere (O<sub>3</sub>, H<sub>2</sub>O<sub>2</sub>, OH *etc.*). Although  
514 some microbial strains from cloud water origin have been shown to metabolize and grow on  
515 culture medium in the presence of H<sub>2</sub>O<sub>2</sub> (Vařtilingom et al., 2013), radical species and their  
516 precursors are reactive compounds and might not easily serve as energy and carbon sources for  
517 microorganisms (Imlay, 2013). Our results on specific metabolic related functions showed that  
518 functions related to methane monooxygenase activity (CH<sub>4</sub> degradation) and hydrogen  
519 peroxide catabolism (H<sub>2</sub>O<sub>2</sub> degradation) were present in air but not in higher proportion than in  
520 other ecosystems (**Fig S3**). Reactive compounds can cause oxidative stress to airborne  
521 microorganisms. In association to adverse physical conditions like UV radiation and  
522 desiccation, oxidative compounds might create more of a physical stress than provide a new  
523 metabolic source for airborne microorganisms. Laboratory investigations of cultivable  
524 microorganisms of an airborne origin showed the presence of particularly resistant strains under  
525 stressful conditions similar to the atmospheric ones (*i.e.* similar UV radiation levels; different  
526 oxidative conditions) (Joly et al., 2015; Yang et al., 2008). However, no study has shown  
527 whether these apparently adapted cells represented the majority of airborne microorganisms.  
528 Since the overall SEED functional classes included mainly metabolic functions, specific stress  
529 related functions using GO (Gene Ontology) terms were also evaluated. We observed that on  
530 average, air showed more stress-related functions (UV response, desiccation and oxidative  
531 stress response related functions) than the other ecosystems due to the higher concentration of  
532 fungi (relatively to bacteria) in air. Thus, when the annotated sequences were separated between  
533 sequences belonging to fungal and bacterial genomes, the bacterial and fungal sequences from  
534 air samples did not show a significantly higher concentration of stress-related functions  
535 compared to the samples coming from other ecosystems (**Fig 4, 5, Fig S4**).

536 Fungal genomes are expected to carry genes associated to global stress-related functions (*i.e.*  
537 UV radiation, desiccation, oxidative stress), because of the innate resistance of fungi especially  
538 fungal spores. These genes associated to global stress-related functions are likely acquired  
539 during sporulation formation and certainly do not result from adaptation of fungi in air. When  
540 studying genes coding more specific proteins that are not associated to spore resistance, such  
541 as lipoate synthase and chromosome plasmid partitioning protein ParA, that might play a role  
542 in oxidative stress (Allary et al., 2007; Bunik, 2003) and are more generally found in stress  
543 resistance and adaptability of microorganisms (Shoeb et al., 2012; Zhang et al., 2018), they  
544 were occasionally found in relatively high concentration in air samples (**Fig S3**). The detection  
545 of metagenomic sequences annotated as genes coding specific proteins in air samples remains  
546 difficult because of the low microbial biomass recovered. That is why we examined the  
547 presence and concentration of global functions (*i.e.* UV protection related functions, oxidative  
548 stress response related functions *etc.*) rather than specific functional genes.

549 The constant and large input of microbial cells to the planetary boundary layer and their  
550 relatively short residence time (a few hours to a few days based on a model assuming that  
551 microbial cells behave like non biological aerosols (Jaenicke, 1980)) might have hindered the  
552 observation of the potential adaptation (physical selection and/or microbial adaptation) of  
553 airborne microorganisms to the stressful atmospheric conditions and to the atmospheric



554 chemicals as discussed above. This issue might be addressed by investigating microbial  
555 functional potential in the free troposphere (preferentially high enough above the ground so as  
556 not to be influenced by the surface) where the microbial fluxes are smaller than in the planetary  
557 boundary layer and where microbial airborne residence time might last much longer than in the  
558 planetary boundary layer. This troposphere approach might help in determining the role of  
559 stress in the atmosphere and validate our conceptual model on the physical stress of microbial  
560 cells taking place during aerosolization and aerial transport selecting the resistant cells (**Fig 6**).  
561 Another explanation might be due to the metagenomic approach that allows to sample both  
562 living and dead cells. Aerosolization has been shown to be particularly stressful and even lethal  
563 for microorganisms (Alsved et al., 2018; Thomas et al., 2011). The functional potential from  
564 the dead cells in air might have a greater weight on the overall functional potential observed  
565 and lead to the dilution of the functional potential of the actual living cells that have adapted to  
566 atmospheric conditions. This might apply for both the overall functional potential discussed  
567 previously and the stress-related functions.

568

## 569 **Conclusion**

570 We conducted the first global comparative metagenomic analysis to characterize the microbial  
571 functional potential signature in the planetary boundary layer. Air samples showed no specific  
572 signature of microbial functional potential which was mainly correlated to the surrounding  
573 landscapes. However, air samples were characterized by a relatively high percentage of fungal  
574 sequences compared to the source ecosystems (soil, surface seawater *etc.*). The relatively higher  
575 concentrations of fungi in air drove the higher proportions of stress-related functions observed  
576 in air metagenomes. Fungal cells and specifically fungal spores are innately resistant entities  
577 well adapted to atmospheric conditions and which might survive better aerosolization and aerial  
578 transport than bacterial cells. Stress-related functions were present in airborne bacteria but  
579 rarely in higher concentrations compared to the bacterial communities in other ecosystems.  
580 However, the constant flux of microbial cells to the planetary boundary layer might have  
581 complicated the determination of a physical selection and/or microbial adaptation of airborne  
582 microorganisms, especially bacterial communities. Meta-omics investigations on air with a  
583 deeper sequencing are needed to confirm our results and explore the functionality of  
584 atmospheric microorganisms further.

585

## 586 **References**

587 Aalismail, N. A., Ngugi, D. K., Díaz-Rúa, R., Alam, I., Cusack, M. and Duarte, C. M.: Functional  
588 metagenomic analysis of dust-associated microbiomes above the Red Sea, *Sci Rep*, 9(1), 1–12,  
589 doi:10.1038/s41598-019-50194-0, 2019.

590 Allary, M., Lu, J. Z., Zhu, L. and Prigge, S. T.: Scavenging of the cofactor lipoate is essential for the  
591 survival of the malaria parasite *Plasmodium falciparum*, *Mol Microbiol*, 63(5), 1331–1344,  
592 doi:10.1111/j.1365-2958.2007.05592.x, 2007.

593 Alsved, M., Holm, S., Christiansen, S., Smidt, M., Ling, M., Boesen, T., Finster, K., Bilde, M.,  
594 Löndahl, J. and Šantl-Temkiv, T.: Effect of Aerosolization and Drying on the Viability of  
595 *Pseudomonas syringae* Cells, *Front Microbiol*, 9, 3086, doi:10.3389/fmicb.2018.03086, 2018.

596 Amato, P., Demeer, F., Melaouhi, A., Fontanella, S., Martin-Biesse, A.-S., Sancelme, M., Laj, P. and  
597 Delort, A.-M.: A fate for organic acids, formaldehyde and methanol in cloud water: their  
598 biotransformation by micro-organisms, *Atmospheric Chemistry and Physics*, 7(15), 4159–4169,  
599 doi:https://doi.org/10.5194/acp-7-4159-2007, 2007.

600 Amato, P., Besaury, L., Joly, M., Penaud, B., Deguillaume, L. and Delort, A.-M.: Metatranscriptomic  
601 exploration of microbial functioning in clouds, *Sci Rep*, 9(1), 1–12, doi:10.1038/s41598-019-41032-4,  
602 2019.

603 Ariya, P., Sun, J., Eltouny, N., Hudson, E., Hayes, C. and Kos, G.: Physical and chemical  
604 characterization of bioaerosols--Implications for nucleation processes, *International Reviews in*  
605 *Physical Chemistry*, 28, 1–32, doi:10.1080/01442350802597438, 2009.

606 Ariya, P. A., Nepotchatykh, O., Ignatova, O. and Amyot, M.: Microbiological degradation of  
607 atmospheric organic compounds, *Geophysical Research Letters*, 29(22), 34–1–34–4,  
608 doi:10.1029/2002GL015637, 2002.

609 Aylor, D. E.: Spread of Plant Disease on a Continental Scale: Role of Aerial Dispersal of Pathogens,  
610 *Ecology*, 84(8), 1989–1997, 2003.

611 Brown, J. K. M. and Hovmöller, M. S.: Aerial dispersal of pathogens on the global and continental  
612 scales and its impact on plant disease, *Science*, 297(5581), 537–541, doi:10.1126/science.1072678,  
613 2002.

614 Brune, A., Frenzel, P. and Cypionka, H.: Life at the oxic–anoxic interface: microbial activities and  
615 adaptations, *FEMS Microbiol Rev*, 24(5), 691–710, doi:10.1111/j.1574-6976.2000.tb00567.x, 2000.

616 Bunik, V. I.: 2-Oxo acid dehydrogenase complexes in redox regulation, *Eur. J. Biochem.*, 270(6),  
617 1036–1042, doi:10.1046/j.1432-1033.2003.03470.x, 2003.

618 Cao, C., Jiang, W., Wang, B., Fang, J., Lang, J., Tian, G., Jiang, J. and Zhu, T. F.: Inhalable  
619 Microorganisms in Beijing’s PM<sub>2.5</sub> and PM<sub>10</sub> Pollutants during a Severe Smog Event, *Environ. Sci.*  
620 *Technol.*, 48(3), 1499–1507, doi:10.1021/es4048472, 2014.

621 Chemidlin Prévost-Bouré, N., Christen, R., Dequiedt, S., Mougél, C., Lelièvre, M., Jolivet, C.,  
622 Shahbazkia, H. R., Guillou, L., Arrouays, D. and Ranjard, L.: Validation and application of a PCR  
623 primer set to quantify fungal communities in the soil environment by real-time quantitative PCR,  
624 *PLoS ONE*, 6(9), e24166, doi:10.1371/journal.pone.0024166, 2011.

625 Delmont, T. O., Malandain, C., Prestat, E., Larose, C., Monier, J.-M., Simonet, P. and Vogel, T. M.:  
626 Metagenomic mining for microbiologists, *ISME J*, 5(12), 1837–1843, doi:10.1038/ismej.2011.61,  
627 2011.

628 Delort, A.-M., Vařtilingom, M., Amato, P., Sancelme, M., Parazols, M., Mailhot, G., Laj, P. and  
629 Deguillaume, L.: A short overview of the microbial population in clouds: Potential roles in  
630 atmospheric chemistry and nucleation processes, *Atmospheric Research*, 98(2), 249–260,  
631 doi:10.1016/j.atmosres.2010.07.004, 2010.

632 Dommergue, A., Amato, P., Tignat-Perrier, R., Magand, O., Thollot, A., Joly, M., Bouvier, L.,  
633 Sellegri, K., Vogel, T., Sonke, J. E., Jaffrezo, J.-L., Andrade, M., Moreno, I., Labuschagne, C., Martin,  
634 L., Zhang, Q. and Larose, C.: Methods to investigate the global atmospheric microbiome, *Front.*  
635 *Microbiol.*, 10, doi:10.3389/fmicb.2019.00243, 2019.

636 Donovan, P. D., Gonzalez, G., Higgins, D. G., Butler, G. and Ito, K.: Identification of fungi in  
637 shotgun metagenomics datasets, *PLOS ONE*, 13(2), e0192898, doi:10.1371/journal.pone.0192898,  
638 2018.

639 Els, N., Larose, C., Baumann-Stanzer, K., Tignat-Perrier, R., Keuschnig, C., Vogel, T. M. and Sattler,  
640 B.: Microbial composition in seasonal time series of free tropospheric air and precipitation reveals  
641 community separation, *Aerobiologia*, doi:10.1007/s10453-019-09606-x, 2019.

642 Fierer, N., Jackson, J. A., Vilgalys, R. and Jackson, R. B.: Assessment of Soil Microbial Community  
643 Structure by Use of Taxon-Specific Quantitative PCR Assays, *Appl. Environ. Microbiol.*, 71(7),  
644 4117–4120, doi:10.1128/AEM.71.7.4117-4120.2005, 2005.

645 Friedl, M. A., McIver, D. K., Hodges, J. C. F., Zhang, X. Y., Muchoney, D., Strahler, A. H.,  
646 Woodcock, C. E., Gopal, S., Schneider, A., Cooper, A., Baccini, A., Gao, F. and Schaaf, C.: Global land  
647 cover mapping from MODIS: algorithms and early results, *Remote Sensing of Environment*, 83(1),  
648 287–302, doi:10.1016/S0034-4257(02)00078-0, 2002.

649 Griffin, D. W.: Atmospheric Movement of Microorganisms in Clouds of Desert Dust and  
650 Implications for Human Health, *Clin Microbiol Rev*, 20(3), 459–477, doi:10.1128/CMR.00039-06,  
651 2007.

652 Gusareva, E. S., Acerbi, E., Lau, K. J. X., Luhung, I., Premkrishnan, B. N. V., Kolundžija, S.,  
653 Purbojati, R. W., Wong, A., Houghton, J. N. I., Miller, D., Gaultier, N. E., Heinle, C. E., Clare, M. E.,  
654 Vettath, V. K., Kee, C., Lim, S. B. Y., Chénard, C., Phung, W. J., Kushwaha, K. K., Nee, A. P., Putra,  
655 A., Panicker, D., Yanqing, K., Hwee, Y. Z., Lohar, S. R., Kuwata, M., Kim, H. L., Yang, L., Uchida, A.,  
656 Drautz-Moses, D. I., Junqueira, A. C. M. and Schuster, S. C.: Microbial communities in the tropical  
657 air ecosystem follow a precise diel cycle, *PNAS*, 116(46), 23299–23308,  
658 doi:10.1073/pnas.1908493116, 2019.

659 Hadley, W. and Winston, C.: Create Elegant Data Visualisations Using the Grammar of Graphics,  
660 [online] Available from: <https://cran.r-project.org/web/packages/ggplot2/ggplot2.pdf>, 2019.

661 Hill, K. A., Shepson, P. B., Galbavy, E. S., Anastasio, C., Kourtev, P. S., Konopka, A. and Stirm, B. H.:  
662 Processing of atmospheric nitrogen by clouds above a forest environment, *Journal of Geophysical*  
663 *Research: Atmospheres*, 112(D11), doi:10.1029/2006JD008002, 2007.

664 Hindré, T., Knibbe, C., Beslon, G. and Schneider, D.: New insights into bacterial adaptation through  
665 *in vivo* and *in silico* experimental evolution, *Nature Reviews Microbiology*, 10(5), 352–365,  
666 doi:10.1038/nrmicro2750, 2012.

667 Huang, M. and Hull, C. M.: Sporulation: How to survive on planet Earth (and beyond), *Curr Genet*,  
668 63(5), 831–838, doi:10.1007/s00294-017-0694-7, 2017.

669 Huerta-Cepas, J., Forslund, K., Coelho, L. P., Szklarczyk, D., Jensen, L. J., von Mering, C. and Bork,  
670 P.: Fast Genome-Wide Functional Annotation through Orthology Assignment by eggNOG-Mapper,  
671 *Mol. Biol. Evol.*, 34(8), 2115–2122, doi:10.1093/molbev/msx148, 2017.

672 Huson, D. H., Richter, D. C., Mitra, S., Auch, A. F. and Schuster, S. C.: Methods for comparative  
673 metagenomics, *BMC Bioinformatics*, 10 Suppl 1, S12, doi:10.1186/1471-2105-10-S1-S12, 2009.

674 Imlay, J. A.: The molecular mechanisms and physiological consequences of oxidative stress: lessons  
675 from a model bacterium, *Nat Rev Microbiol*, 11(7), 443–454, doi:10.1038/nrmicro3032, 2013.

676 Innocente, E., Squizzato, S., Visin, F., Facca, C., Rampazzo, G., Bertolini, V., Gandolfi, I., Franzetti,  
677 A., Ambrosini, R. and Bestetti, G.: Influence of seasonality, air mass origin and particulate matter  
678 chemical composition on airborne bacterial community structure in the Po Valley, Italy, *Sci. Total*  
679 *Environ.*, 593–594, 677–687, doi:10.1016/j.scitotenv.2017.03.199, 2017.

680 Jaenicke, R.: Atmospheric aerosols and global climate, *Journal of Aerosol Science*, 11(5), 577–588,  
681 doi:10.1016/0021-8502(80)90131-7, 1980.

682 Joly, M., Amato, P., Sancelme, M., Vinatier, V., Abrantes, M., Deguillaume, L. and Delort, A.-M.:  
683 Survival of microbial isolates from clouds toward simulated atmospheric stress factors, *Atmospheric*  
684 *Environment*, 117, 92–98, doi:10.1016/j.atmosenv.2015.07.009, 2015.

685 Li, Y., Zheng, L., Zhang, Y., Liu, H. and Jing, H.: Comparative metagenomics study reveals pollution  
686 induced changes of microbial genes in mangrove sediments, *Scientific Reports*, 9(1), 5739,  
687 doi:10.1038/s41598-019-42260-4, 2019.

688 Malik, A. A., Chowdhury, S., Schlager, V., Oliver, A., Puissant, J., Vazquez, P. G. M., Jehmlich, N.,  
689 von Bergen, M., Griffiths, R. I. and Gleixner, G.: Soil Fungal:Bacterial Ratios Are Linked to Altered  
690 Carbon Cycling, *Front. Microbiol.*, 7, doi:10.3389/fmicb.2016.01247, 2016.

691 Oksanen, J., Guillaume Blanchet, F., Friendly, M., Kindt, R., Legendre, P., McGlinn, D., Minchin, P.  
692 R., O'Hara, R. B., Simpson, G. L., Solymos, P., Stevens, M. H. H., Szoecs, E. and Wagner, H.:  
693 Community Ecology Package, [online] Available from: <https://github.com/vegandevs/vegan>, 2019.

694 Rey, O., Danchin, E., Mirouze, M., Loot, C. and Blanchet, S.: Adaptation to Global Change: A  
695 Transposable Element–Epigenetics Perspective, *Trends in Ecology & Evolution*, 31(7), 514–526,  
696 doi:10.1016/j.tree.2016.03.013, 2016.

697 Shannan, S., Collins, K. and Emanuel, W. R.: Global mosaics of the standard MODIS land cover type  
698 data, 2014.

699 Shoeb, E., Badar, U., Akhter, J., Shams, H., Sultana, M. and Ansari, M. A.: Horizontal gene transfer  
700 of stress resistance genes through plasmid transport, *World J. Microbiol. Biotechnol.*, 28(3), 1021–  
701 1025, doi:10.1007/s11274-011-0900-6, 2012.

702 Thomas, R. J., Webber, D., Hopkins, R., Frost, A., Laws, T., Jayasekera, P. N. and Atkins, T.: The  
703 Cell Membrane as a Major Site of Damage during Aerosolization of *Escherichia coli*, *Appl. Environ.*  
704 *Microbiol.*, 77(3), 920–925, doi:10.1128/AEM.01116-10, 2011.

705 Tignat-Perrier, R., Dommergue, A., Thollot, A., Keuschnig, C., Magand, O., Vogel, T. M. and  
706 Larose, C.: Global airborne microbial communities controlled by surrounding landscapes and wind  
707 conditions, *Sci Rep*, 9(1), 1–11, doi:10.1038/s41598-019-51073-4, 2019.

708 Tringe, S. G., von Mering, C., Kobayashi, A., Salamov, A. A., Chen, K., Chang, H. W., Podar, M.,  
709 Short, J. M., Mathur, E. J., Detter, J. C., Bork, P., Hugenholtz, P. and Rubin, E. M.: Comparative  
710 metagenomics of microbial communities, *Science*, 308(5721), 554–557, doi:10.1126/science.1107851,  
711 2005.

712 Vaitilingom, M., Amato, P., Sancelme, M., Laj, P., Leriche, M. and Delort, A.-M.: Contribution of  
713 Microbial Activity to Carbon Chemistry in Clouds, *Appl Environ Microbiol*, 76(1), 23–29,  
714 doi:10.1128/AEM.01127-09, 2010.

715 Vaitilingom, M., Deguillaume, L., Vinatier, V., Sancelme, M., Amato, P., Chaumerliac, N. and Delort,  
716 A.-M.: Potential impact of microbial activity on the oxidant capacity and organic carbon budget in  
717 clouds, *PNAS*, 110(2), 559–564, doi:10.1073/pnas.1205743110, 2013.

718 Vartoukian, S. R., Palmer, R. M. and Wade, W. G.: Strategies for culture of 'unculturable' bacteria,  
719 *FEMS Microbiology Letters*, 309(1), 1–7, doi:10.1111/j.1574-6968.2010.02000.x, 2010.

720 Wickham, H.: Flexibly Reshape Data: A Reboot of the Reshape Packa, [online] Available from:  
721 <https://cran.r-project.org/web/packages/reshape2/reshape2.pdf>, 2017.

722 Wood, D. E. and Salzberg, S. L.: Kraken: ultrafast metagenomic sequence classification using exact  
723 alignments, *Genome Biology*, 15(3), R46, doi:10.1186/gb-2014-15-3-r46, 2014.

724 Xie, W., Wang, F., Guo, L., Chen, Z., Sievert, S. M., Meng, J., Huang, G., Li, Y., Yan, Q., Wu, S.,  
725 Wang, X., Chen, S., He, G., Xiao, X. and Xu, A.: Comparative metagenomics of microbial  
726 communities inhabiting deep-sea hydrothermal vent chimneys with contrasting chemistries, *The*  
727 *ISME Journal*, 5(3), 414–426, doi:10.1038/ismej.2010.144, 2011.

728 Yang, Y., Yokobori, S. and Yamagishi, A.: UV-resistant bacteria isolated from upper troposphere and  
729 lower stratosphere, *Biol.Sci.Space*, 22, doi:10.2187/bss.22.18, 2008.

730 Yooseph, S., Nealson, K. H., Rusch, D. B., McCrow, J. P., Dupont, C. L., Kim, M., Johnson, J.,  
731 Montgomery, R., Ferriera, S., Beeson, K., Williamson, S. J., Tovchigrechko, A., Allen, A. E., Zeigler,  
732 L. A., Sutton, G., Eisenstadt, E., Rogers, Y.-H., Friedman, R., Frazier, M. and Venter, J. C.: Genomic  
733 and functional adaptation in surface ocean planktonic prokaryotes, *Nature*, 468(7320), 60–66,  
734 doi:10.1038/nature09530, 2010.

735 Yooseph, S., Andrews-Pfannkoch, C., Tenney, A., McQuaid, J., Williamson, S., Thiagarajan, M.,  
736 Bami, D., Zeigler-Allen, L., Hoffman, J., Goll, J. B., Fadrosch, D., Glass, J., Adams, M. D., Friedman,  
737 R. and Venter, J. C.: A Metagenomic Framework for the Study of Airborne Microbial Communities,  
738 *PLOS ONE*, 8(12), e81862, doi:10.1371/journal.pone.0081862, 2013.

739 Zhang, H., Hu, Y., Zhou, C., Yang, Z., Wu, L., Zhu, M., Bao, H., Zhou, Y., Pang, M., Wang, R. and  
740 Zhou, X.: Stress resistance, motility and biofilm formation mediated by a 25kb plasmid pLMSZ08 in  
741 *Listeria monocytogenes*, *Food Control*, 94, 345–352, doi:10.1016/j.foodcont.2018.07.002, 2018.

742

743 **Competing interests.** The authors declare that they have no conflict of interest.

744

745 **Financial support.** This work was supported by the Agence Nationale de la Recherche  
746 [ANR-15-CE01-0002–03 INHALE]; Région Auvergne-Rhône Alpes [ARC3 2016];  
747 CAMPUS France [program XU GUANGQI] and the French Polar Institute IPEV [program  
748 1028 and 399].

749

750 **Author contributions.** AD, CL and TMV designed the experiment. RTP, AD, AT and OM  
751 conducted the sampling field campaign. RTP did the molecular biology, bioinformatics and  
752 statistical analyses. RTP, AD, CL and TMV analyzed the results. RTP, TM, AD and CL wrote  
753 the manuscript. All authors reviewed the manuscript.

754

755 **Acknowledgements.** The chemical analyses were performed at the IGE AirOSol platform. This  
756 work was hosted by the following stations: Chacaltaya, Namco, puy de Dôme, Cape-Point, Pic-  
757 du-Midi, Amsterdam-Island, Storm-Peak, Villum RS and we thank I.Jouvie, G.Hallar,  
758 I.McCubbin, Benny and Jesper, B.Jensen, A.Nicosia, M.Ribeiro, L.Besaury, L.Bouvier,  
759 M.Joly, I.Moreno, M.Rocca, F.Velarde for sampling and station management. We thank our  
760 project partners: K.Sellegrì, P.Amato, M.Andrade, Q.Zhang, C.Labuschagne and L.Martin, J.  
761 Sonke. We thank R.Edwards, J. Schauer and C.Worley for lending their HV sampler. We thank  
762 L.Pouilloux for computing assistance and maintenance of the Newton server.

763

764 **Data availability.** Sequences reported in this paper have been deposited in [ftp://ftp-adn.ec-lyon.fr/Tignat-Perrier\\_2020\\_air\\_metagen\\_INHALE/](ftp://ftp-adn.ec-lyon.fr/Tignat-Perrier_2020_air_metagen_INHALE/). A file has been attached explaining the  
765 correspondence between file names and samples.  
766